COMPUTER VISION, GRAPHICS, AND IMAGE PROCESSING 29, 1–12 (1985)

Tracing Planar Surface Motion from a Projection without Knowing the Correspondence

KEN-ICHI KANATANI

Department of Computer Science, Gunma University, Kiryu, Gunma 376, Japan

Received June 30, 1983; revised June 4, 1984

The 3-dimensional motion of a planar surface is detected only from the motion of its projected 2-dimensional contour image on the plane of vision. There is no need to know the correspondence of points. The motion is explicitly given by measuring "diameters" of the image contour on the plane of vision. No iterative or matching processes are involved. Numerical examples are also given.

1. INTRODUCTION

Detecting the 3-dimensional motion of a surface from the 2-dimensional motion of its projected image is one of the most important tasks or "modules" of computer vision and image processing. One of the prevailing approaches is first to detect the "correspondence," i.e., the knowledge of which point moves to which one, and to analyze the "optical flow" (e.g., [1, 2, 3]). For example, if the surface is a face of a polyhedron, the correspondence is determined by detecting edges and corners. In general, however, determination of correspondence is a time consuming process involving iterative searches. Moreover, if the surface is not a polygon but an arbitrary smooth shape, no correspondence could be known at all. Even if the correspondence is known, the computation of the motion could become complicated. Translational motions must be separated from rotational motions (cf. [1, 2]). Furthermore, the accuracy depends greatly on the choice of the points used for computation. If those points are located very near each other, a small amount of noise would make the computational error very great, so that some kind of correction like averaging over different correspondences is necessary (e.g., [3]).

In view of this, a technique to detect the 3-dimensional motion without knowing the correspondence is desired. It is also desired that measurement involve data just enough to know the desired component of the motion. For example, if the orientation of the surface is wanted, the involved data should be "invariant" with respect to translational motions. Besides, the necessary computation should be as simple as possible, preferably without any iterative searches. In this paper, we present such a technique. We present a set of "explicit" formulae to compute the surface motion from a small number of measured "features" alone. The image can be erased out of the memory once the features are obtained, for there is no need to compare or correlate two images. This saves the memory space. Similar approaches have already been seen. For example, Amari [4, 5] proposed a theory of invariant features to detect the motion of gray-level images. Kanatani [6] applied a mathematical principle called "integral geometry" or "stereology" [7–12] to detect the orientation of an infinitely large plane surface with a texture on it. Here we do not need any texture at all. Only necessary is the assumption that the surface is "planar," having a "closed contour."

0734-189X/85 $3.00

The iterative search is one of the basic techniques in image processing. It is most universal in the sense that it can be applied to any problems, for its principle is to test feasible possibilities systematically to reach one which best matches the given requirement. At the price of universality, however, it usually involves much computation time, and the process sometimes does not converge to the true solution, especially when the cost function has local maxima or minima. In order to accelerate or ensure convergence, a very good approximation is necessary as an initial guess. Thus, it is of vital importance to obtain an "explicit" scheme without involving iterative searches even though it gives only an approximation. The presented estimation technique is rough in the sense that it involves various approximations. Another scheme similar to this but exact in principle is also proposed by Kanatani [13]. It involves numerical integration of certain functions on the plane of vision, but the accuracy depends sensitively on the choice of these functions. The estimation is very accurate when the motion is small but cannot be applied when the motion is large, while the present one gives a fairly good estimation even if the motion is large, as is illustrated in our examples. Thus, the virtues of these two methods are complementary, and the present one will serve many purposes if appropriately used.

2. SPECIFICATION OF SURFACE ORIENTATION AND ROTATION

In this paper, we consider only the orthographic projection. (The scheme of Kanatani [13] is applicable to the perspective projection.) Hence, the location of the surface is irrelevant, and we adopt the convention that it passes through the origin of the space and that we are viewing the image orthographically projected along the z axis onto the xy plane. There are several ways, mutually equivalent, of describing the surface orientation. One obvious way is to specify the unit normal vector (n_1, n_2, n_3). Since (n_1, n_2, n_3) and $(-n_1, -n_2, -n_3)$ describe the same orientation, we can always assume $n_3 > 0$. We exclude the exceptional case of $n_3 = 0$ (i.e., the surface is orthogonal to the plane of vision.) The equation of the surface has the form $n_1x + n_2y + n_3z = 0$. Alternatively, we can use the spherical coordinates σ and τ of the normal (Fig. 1). It follows by our convention that $0 \leq \sigma < \pi/2$ and $0 \leq \tau < 2\pi$. The parameter σ is termed the "slant" and τ the "tilt" of the surface. We can alternatively use the "gradients" (p, q), where $p = \partial z/\partial x$ and $q = \partial z/\partial y$. The surface equation is then expressed by $z = px + qy$.

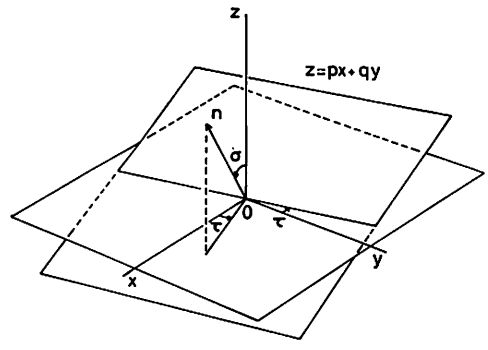

FIG. 1. Specification of surface orientation by the normal vector $\boldsymbol{n}$, the slant σ and tilt τ, and the gradients (p, q).

These three descriptions are mutually equivalent and related to each other as follows:

(i) *normal vs. slant-tilt*

$$n_1 = \sin\sigma\cos\tau, \qquad n_2 = \sin\sigma\sin\tau, \qquad n_3 = \cos\sigma, \tag{2.1}$$

$$\sigma = \cos^{-1}n_3, \qquad \tau = \tan^{-1}(n_2/n_1), \tag{2.2}$$

where appropriate branches of $\cos^{-1}$ and $\tan^{-1}$ must be chosen by considering the signs of n_1, n_2, and n_3.

(ii) *slant-tilt vs. gradients*

$$p = -\tan\sigma\cos\tau, \qquad q = -\tan\sigma\sin\tau, \tag{2.3}$$

$$\sigma = \tan^{-1}\sqrt{p^2 + q^2}, \qquad \tau = \tan^{-1}(q/p), \tag{2.4}$$

where again appropriate branches of $\tan^{-1}$ must be chosen by considering the signs of p and q.

(iii) *gradients vs. normal*

$$p = -n_1/n_3, \qquad q = -n_2/n_3, \tag{2.5}$$

$$n_1 = -p/\sqrt{p^2 + q^2 + 1}, \qquad n_2 = -q/\sqrt{p^2 + q^2 + 1}, \qquad n_3 = 1/\sqrt{p^2 + q^2 + 1}. \tag{2.6}$$

Let $(\omega_1, \omega_2, \omega_3)$ be the angular velocity vector, which describes an instantaneous rotation of angular velocity $\omega = \sqrt{\omega_1^2 + \omega_2^2 + \omega_3^2}$ around an axis of direction cosine$(\omega_1, \omega_2, \omega_3)/\omega$ through the origin. Then, the time change of the surface orientation is described by one of the following three sets of differential equations:

$$\begin{cases} dn_1/dt = n_3\omega_2 - n_2\omega_3, \\ dn_2/dt = -n_3\omega_1 + n_1\omega_3, \\ dn_3/dt = n_2\omega_1 - n_1\omega_2; \end{cases} \tag{2.7}$$

$$\begin{cases} d\sigma/dt = -\omega_1\sin\tau + \omega_2\cos\tau, \\ d\tau/dt = \omega_3 - (\omega_1\cos\tau + \omega_2\sin\tau)/\tan\sigma; \end{cases} \tag{2.8}$$

$$\begin{cases} dp/dt = pq\omega_1 - (p^2 + 1)\omega_2 - q\omega_3, \\ dq/dt = (q^2 + 1)\omega_1 - pq\omega_2 + p\omega_3. \end{cases} \tag{2.9}$$

This surface motion induces, by projection, the "velocity field" or the "optical flow" in the xy plane as follows:

$$\begin{aligned} dx/dt &= p\omega_2 x + (q\omega_2 - \omega_3)y, \\ dy/dt &= -(p\omega_1 - \omega_3)x - q\omega_1 y, \end{aligned} \tag{2.10}$$

3. DISTRIBUTION DENSITY AND FEATURES

Now, the only assumption here is that the surface is planar, having a closed contour. Hence, all relevant information must be extracted from the circumference contour alone. This means that the surface itself can be an infinite plane on which a closed curve is drawn. This does not make any difference, because we are looking at the curve image alone. A closed curve on the plane of vision has a number of characteristics—the length, the area, the center of gravity, the moments, etc. What we consider here is the "distribution density" $f(\theta)$ of the contour. It is defined as follows: Let the closed curve be disected into infinitesimally small line segments of length $\mathrm{d}l$. The orientation of each line segment is described by angle θ made from the x axis. Since θ and $\theta + \pi$ describe the same orientation, we choose one of the two possibilities randomly with probability $\frac{1}{2}$. The distribution density $f(\theta)$ is defined so that $f(\theta)\,\mathrm{d}\theta$ is the total length of those line segments of orientation between θ and $\theta + \mathrm{d}\theta$. By definition, $f(\theta)$ is "symmetric" in the sense that $f(\theta) = f(\theta + \pi)$, and $\int_0^{2\pi} f(\theta)\,\mathrm{d}\theta$ is the total length of the curve.

The above definition is merely a mathematical conception, and we do not compute $f(\theta)$ by this definition. What we measure is the "diameter" $D(\theta)$ of the contour, i.e., the distance between the two parallel lines of orientation θ tangent to the contour, as is indicated in Fig. 2. Hence, $D(\theta)$ is a symmetric function, $D(\theta) = D(\theta + \pi)$, defined for $0 \leq \theta < 2\pi$. In contrast to the distribution density, the diameter can be measured easily for any particular θ directly on the plane of vision. Yet, there is a mathematical relation between them. Suppose the contour is convex. Then, we have the following theorem.

THEOREM

$$D(\theta) = \frac{1}{2}\int_0^{2\pi} |\sin(\theta - \theta')| f(\theta')\,\mathrm{d}\theta'. \tag{3.1}$$

Proof. Let S be the area of the plane of vision. Put a line of orientation θ on it randomly and consider the expected number of intersections with the curve. Consider those line segments of length $\mathrm{d}l$ whose orientations are between θ' and $\theta' + \mathrm{d}\theta'$. Such a line segment intersects the line when its center falls inside the area of width $|\sin(\theta - \theta')|$ along the line (Fig. 3). Since there are $f(\theta')\,\mathrm{d}\theta'/S\,\mathrm{d}l$ such line segments per unit area, $|\sin(\theta - \theta')| f(\theta')\,\mathrm{d}\theta'/S$ of them intersect the line per unit length. Hence, the expected number of intersections per unit length is $\int_0^{2\pi} |\sin(\theta$

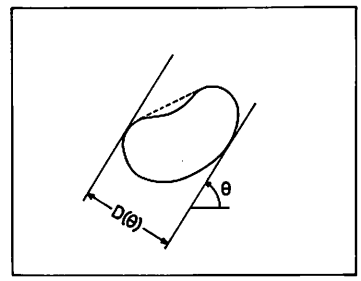

FIG. 2. Diameter $D(\theta)$ is the distance between the two parallel tangent lines of orientation θ.

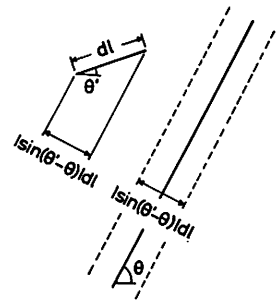

FIG. 3. A line segment intersects the line when its center falls inside the area of width $|\sin(\theta' - \theta)|$ along the line.

$-\theta')|f(\theta')\,d\theta'/S$. On the other hand, the expectation over random droppings is equivalent to considering parallel lines of infinitesimally small spacing dh and of orientation θ covering the plane of vision [7–9]. The total length is S/dh, and the total number of intersections is $2D(\theta)/dh$, one line intersecting the curve twice due to the convexity of the curve. (We need not consider the tangent lines, because they arise with "measure 0.") Hence, the number of intersections per unit length is $2D(\theta)/S$, which proves the theorem. □

The transform of Eq. (3.1) was generalized to include 3-dimensional figures not necessarily curves by Kanatani [10], who termed it the "Buffon transform" and gave it a tensor formulation invariant to coordinate transformations (see also Kanatani [14]). He also gave a procedure of inverting the transform of (3.1). Let $D(\theta)$ be expanded in the Fourier series

$$D(\theta) = \frac{C}{2\pi}\left[1 + \sum_{n=2}^{\infty}{}'(A_n\cos n\theta + B_n\sin n\theta)\right], \tag{3.2}$$

where Σ' denotes summation with respect to even numbers. The odd terms do not appear due to the symmetry of $D(\theta)$. Then, the distribution density $f(\theta)$ is given by

$$f(\theta) = \frac{C/2}{2\pi}\left[1 - \sum_{n=2}^{\infty}{}'(n^2 - 1)(A_n\cos n\theta + B_n\sin n\theta)\right]. \tag{3.3}$$

(A formal proof of this requires the orthogonality of irreducible representations of the 2-dimensional rotation group and Schur's lemma. See Kanatani [10].) If D_k is the diameter for $\theta = \pi k/N, k = 0, 1, \ldots, N$, the Fourier coefficients in Eq. (3.2) are approximated by

$$C = 2\pi\sum_{k=0}^{N-1} D_k/N, \tag{3.4}$$

$$A_n = 2\sum_{k=0}^{N-1} D_k\cos(n\pi k/N)\Big/\sum_{k=0}^{N-1} D_k, \qquad B_n = 2\sum_{k=0}^{N-1} D_k\sin(n\pi k/N)\Big/\sum_{k=0}^{N-1} D_k. \tag{3.5}$$

As is shown in the next section, only C, A_2 and B_2 are sufficient to determine the 3-dimensional motion. So far we have assumed that the surface contour is convex, but we can remove this assumption. As can be seen from Fig. 3, if we measure the diameter $D(\theta)$ of a nonconvex contour from outside, we are actually measuring the diameter of its "convex hull," i.e., the minimum convex domain containing the contour. An important fact is that the convex hull is "invariant" with respect to (not necessarily orthographic) projections. In other words, the convex hull of the projected image is the same as the projected image of the convex hull of the original contour. This is apparent because "tangency" is an invariant concept with respect to projections. Hence, we have only to regard the convex hull as the "real surface."

4. DETERMINATION OF SURFACE MOTION FROM FEATURES

Suppose we observe a 2-dimensional image of a moving contour at some time t. An approximation we adopt here is to assume that the distribution density of the contour image has the form

$$f(\theta) = \frac{c}{2\pi}[1 + a_2\cos 2\theta + b_2\sin 2\theta], \tag{4.1}$$

and that the higher harmonics can be neglected. On the plane of vision is induced the velocity field of Eqs. (2.10). Due to this velocity field, the coefficients of Eq. (4.1) are not constants but functions of time. Their time derivatives become

$$\mathrm{d}c/\mathrm{d}t = -\tfrac{1}{4}c[b_2 p - (a_2 - 2)q]\omega_1 + \tfrac{1}{4}c[(a_2 + 2)p + b_2 q]\omega_2, \tag{4.2}$$

$$\mathrm{d}a_2/\mathrm{d}t = \tfrac{1}{4}[b_2(4 + a_2)p + (6 - a_2^2)q]\omega_1 + \tfrac{1}{4}[(6 - a_2^2)p + b_2(4 - a_2)q]\omega_2 - 2b_2\omega_3, \tag{4.3}$$

$$\mathrm{d}b_2/\mathrm{d}t = \tfrac{1}{4}[(b_2^2 - 4a_2 - 6)p - a_2 b_2 q]\omega_1 - \tfrac{1}{4}[a_2 b_2 p + (b_2^2 + 4a_2 - 6)q]\omega_2 + 2a_2\omega_3, \tag{4.4}$$

(The mathematical principles to derive this result are discussed in Kanatani [6, 10].) If we compare Eq. (3.3) and Eq. (4.1), we can see

$$c = C/2 \qquad a_2 = -3A_2, \qquad b_2 = -3B_2, \tag{4.5}$$

and hence the transformation of the "features" C, A_2 and B_2 due to the motion are obtained. The relevant equations become

$$\frac{1}{C}\frac{\mathrm{d}C}{\mathrm{d}t} = \left[-\frac{3}{4}B_2 p + \frac{1}{2}(1 + 3A_2)q\right]\omega_1 + \left[\frac{1}{2}(1 - 3A_2)p - \frac{3}{4}B_2 q\right]\omega_2, \tag{4.6}$$

$$\mathrm{d}A_2/\mathrm{d}t = [B_2(1 - \tfrac{3}{4}A_2)p - (\tfrac{1}{2} - \tfrac{3}{4}A_2^2)q]\omega_1 + [-(\tfrac{1}{2} - \tfrac{3}{4}A_2^2)p + B_2(1 + \tfrac{3}{4}A_2)q]\omega_2 - 2B_2\omega_3, \tag{4.7}$$

$$\mathrm{d}B_2/\mathrm{d}t = [(\tfrac{1}{2} - A_2 - \tfrac{3}{4}B_2^2)p + \tfrac{3}{4}A_2 B_2 q]\omega_1 + [\tfrac{3}{4}A_2 B_2 p - (\tfrac{1}{2} - A_2 - \tfrac{3}{4}B_2^2)q]\omega_2 + 2A_2\omega_3. \tag{4.8}$$

Equations (4.6)–(4.8) are viewed as a set of simultaneous linear equations for the angular velocity vector $(\omega_1, \omega_2, \omega_3)$. The solution is given in the form

$$\begin{bmatrix}\omega_1\\ \omega_2\end{bmatrix} = \frac{4}{B_2(q^2-p^2)+2A_2pq}\left[\frac{1}{2}\left((A,\dot{A})\Big/\left(\frac{2}{3}-\|A\|^2\right)-\dot{C}/C\right)\begin{bmatrix}A_2p+B_2q\\ B_2p-A_2q\end{bmatrix}\right.$$
$$\left.+(A,\dot{A})\Big/\left(\frac{2}{3}-\|A\|^2\right)\begin{bmatrix}p\\ q\end{bmatrix}\right], \tag{4.9}$$

$$\omega_3 = \frac{1}{2\|A\|^2}\left[[A,\dot{A}]+\left(\left(\|A\|^2-\frac{1}{2}A_2\right)p-\frac{1}{2}B_2q\right)\omega_1\right.$$
$$\left.+\left(-\frac{1}{2}B_2p+\left(\|A\|^2+\frac{1}{2}A_2\right)q\right)\omega_2\right], \tag{4.10}$$

where the following abbreviations are employed:

$$\|A\| = \sqrt{A_2^2+B_2^2}, \tag{4.11}$$

$$(A,\dot{A}) = A_2\mathrm{d}A_2/\mathrm{d}t + B_2\mathrm{d}B_2/\mathrm{d}t, \qquad [A,\dot{A}] = A_2\mathrm{d}B_2/\mathrm{d}t - B_2\mathrm{d}A_2/\mathrm{d}t, \tag{4.12}$$

and $\dot{C} = \mathrm{d}C/\mathrm{d}t$. Here, C, A_2 and B_2 can be measured at each time. Their time derivatives are approximated by measuring them at time t and time $t+\Delta t$, a sufficiently short time later, and taking the difference. For example, $\mathrm{d}A_2/\mathrm{d}t \simeq [A_2(t+\Delta t)-A_2(t)]/\Delta t$. Hence, once we know the gradients (p,q) at time t, we can compute the angular velocity vector $(\omega_1, \omega_2, \omega_3)$ by these equations. Then, in view of Eqs. (2.9), the gradients (p',q') at time $t+\Delta t$ can be approximated by

$$p' \simeq p + [pq\omega_1 - (p^2+1)\omega_2 - q\omega_3]\Delta t, \tag{4.13}$$

$$q' \simeq q + [(q^2+1)\omega_1 - pq\omega_2 + p\omega_3]\Delta t, \tag{4.14}$$

or equivalently from Eqs. (2.7) or (2.8). It then follows that, if we know the initial orientation of the surface, we can trace the surface orientation, successively applying the above procedure. However, as is seen from Eq. (4.9), this scheme fails to work if $p = q = 0$ at time t. In this case, we need a different scheme, which will be presented later.

5. A NUMERICAL EXAMPLE OF TRACING SURFACE ORIENTATION

Figure 4 shows projected contour images of a moving planar surface in the space. The slant and tilt of C_0 are 60° and 80°, respectively, or in terms of the gradients $p = -0.306$ and $q = -1.706$, and C_1, C_2, and C_3 are images of the same surface after being rotated by 10°, 20°, and 30°, respectively, about an axis of direction cosine $(1/\sqrt{3}, 1/\sqrt{3}, 1/\sqrt{3})$. The transition of surface orientation is described by a "trajectory" in the pq plane, or the "gradient space." Figure 5 shows the true (solid) and a computed (dashed) trajectories, where we computed the features C, A_2, and B_2 from diameters of 18 different orientations. The precision is remarkable in view of the fairly large amount of relative motions and the involved approximations.

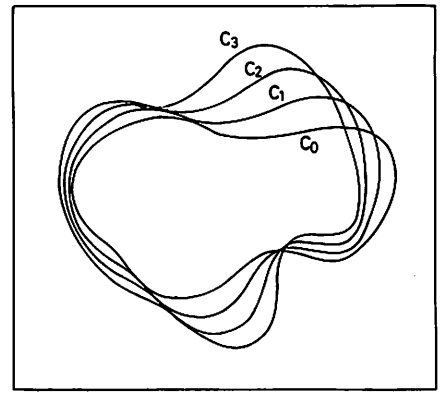

FIG. 4. Projected images of a surface: C_0 has slant 60° and tilt 80°. C_1, C_2, and C_3 are the images after rotations of 10°, 20° and 30°, respectively, about an axis of direction cosine $(1/\sqrt{3}, 1/\sqrt{3}, 1/\sqrt{3})$.

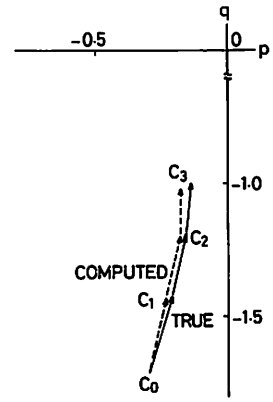

FIG. 5. The true (solid) and the computed (dashed) trajectories of the surface orientation for the images in Fig. 4.

In the course of computation, we employed a few modifications. The first one is related to the fact that, if p and q are small, the angular velocities ω_1 and ω_2 exert only a small distortion rate, while ω_3, the angular velocity about the z axis, induces a 2-dimensional rotation whose distortion rate is of order 1 (see Eqs. (2.10)). Hence, we proceeded as follows: If $p, q \simeq 0$ in Eq. (4.10), we have $\omega_3 \simeq [\mathbf{A}, \dot{\mathbf{A}}]/2\|\mathbf{A}\|^2$. Let $\bar{\omega}_3$ be this value. Using it as a first approximation, we first rotate the image at time $t + \Delta t$ by $-\bar{\omega}_3 \Delta t$. This is easily done by rewriting the features as $C \to C, A_2 \to A_2\cos(\bar{\omega}_3 \Delta t) + B_2\sin(\bar{\omega}_3 \Delta t), B_2 \to -A_2\sin(\bar{\omega}_3 \Delta t) + B_2\cos(\bar{\omega}_3 \Delta t)$ at time $t + \Delta t$. (We do not have to change the image itself.) Then, this modified motion is expected to have a smaller value of ω_3. After computing the gradients (p', q') at $t + \Delta t$ by the procedure described previously, we obtain the true gradients by transformation $p' \to p'\cos(\bar{\omega}_3 \Delta t) - q'\sin(\bar{\omega}_3 \Delta t)$, $q' \to p'\sin(\bar{\omega}_3 \Delta t) + q'\cos(\bar{\omega}_3 \Delta t)$.

The second one is the use of the normal vector instead of the gradients. If p and q are given, the normal vector is given by Eqs. (2.6). Given the angular velocity vector $(\omega_1, \omega_2, \omega_3)$, we can compute the normal vector at time $t + \Delta t$ by using Eqs. (2.7), and the gradients are given by Eqs. (2.5). Of course, Eqs. (2.7), (2.8), and (2.9) are

mathematically equivalent to each other as differential equations, but Eqs. (2.7) seem to give a better solution when approximated as difference equations with derivatives replaced by simple differences, especially when p and q are small.

6. THE CASE OF $p = q = 0$

As was mentioned earlier, we need a different scheme when $p = q = 0$ at time t, in which case angular velocities ω_1 and ω_2 do not affect the image (see Eqs. (2.10)). Since the velocity describes an instantaneous "linear" approximation of the motion, we must have a higher order approximation when the velocity vanishes. Suppose $p = q = 0$ at time t, and let (p', q') be the gradients a short time later at time t'. Then, the transformation on the plane of vision has the following form: point (x, y) at time t moves to point(x', y'), where

$$\begin{aligned} x' &= (1 - p'^2/2)x - (p'q' + \Omega)y + O(p'^4, q'^4, \Omega^2), \\ y' &= -(p'q' - \Omega)x + (1 - p'^2/2)y + O(p'^4, q'^4, \Omega^2). \end{aligned} \tag{6.1}$$

Here, the last terms designate those of order p'^4, q'^4 or Ω^2, and Ω is an arbitrary angle of rotation about the z axis. In order that these equations have a practical sense, the magnitude of the "in-plane rotation" Ω must be small and have the order of p'^2 or q'^2.

If the distribution density of the contour curve is given by Eqs. (4.1) at time t, then it becomes at time t'

$$f(\theta) = \frac{c'}{2\pi}\left[1 + a_2'\cos 2\theta + b_2'\sin 2\theta + a_4'\cos 4\theta + b_4'\sin 4\theta\right] + O(p'^4, q'^4, \Omega^2), \tag{6.2}$$

where

$$c' = c\left[1 + \tfrac{1}{4}p'^2 + \tfrac{1}{8}\left((q'^2 - p'^2)a_2 - 2p'q'b_2\right)\right], \tag{6.3}$$

$$a_2' = a_2 + \tfrac{3}{4}(q'^2 - p'^2) - \tfrac{1}{8}a_2\left[(q'^2 - p'^2)a_2 - 2b_2 p'q'\right] - 2b_2\Omega, \tag{6.4}$$

$$b_2' = b_2 - \tfrac{3}{4}(2p'q') - \tfrac{1}{8}b_2\left[(q'^2 - p'^2)a_2 - 2b_2 p'q'\right] + 2a_2\Omega, \tag{6.5}$$

$$a_4' = \tfrac{5}{8}\left[(q'^2 - p'^2)a_2 + 2p'q'b_2\right], \tag{6.6}$$

$$b_4' = \tfrac{5}{8}\left[(q'^2 - p'^2)b_2 - 2p'q'a_2\right], \tag{6.7}$$

(The mathematical principles to derive this result are discussed in Kanatani [6, 10].) From Eqs. (6.3), (6.4), and (6.5) and relations (4.5), we can also solve for p', q' and Ω in terms of C, C', A_2, A_2', B_2 and B_2' as follows. First, p' and q' are given as the solution of

$$\begin{aligned} &A_2(q'^2 - p'^2) - 2B_2 pq = -\tfrac{8}{3}(1 - C'/C), \\ &p'^2 + q'^2 = 4\left[1 - C'/C + \left((\mathbf{A}, \mathbf{A}') - \|\mathbf{A}\|^2\right)/\left(\tfrac{2}{3} - \|\mathbf{A}\|^2\right)\right], \end{aligned} \tag{6.8}$$

and Ω is given by

$$\Omega = \left([\mathbf{A}, \mathbf{A}'] - \tfrac{1}{4}\left[B_2(q'^2 - p'^2) + 2A_2pq\right]\right)/2\|\mathbf{A}\|^2, \tag{6.9}$$

where we have used abbreviations

$$(\mathbf{A}, \mathbf{A}') = A_2A_2' + B_2B_2', \qquad [\mathbf{A}, \mathbf{A}'] = A_2B_2' - B_2A_2'. \tag{6.10}$$

If we put

$$p' = r\cos\phi, \qquad q' = r\sin\phi, \tag{6.11}$$

and define ϕ_0 to be the angle given by

$$\cos 2\phi_0 = A_2/\|\mathbf{A}\|, \qquad \sin 2\phi_0 = B_2/\|\mathbf{A}\|, \tag{6.12}$$

The solution of Eqs. (6.8) is given as

$$r = 2\sqrt{1 - C'/C + \left((\mathbf{A}, \mathbf{A}') - \|\mathbf{A}\|^2\right)/\left(\tfrac{2}{3} - \|\mathbf{A}\|^2\right)}, \tag{6.13}$$

$$\phi = \phi_0 + \tfrac{1}{2}\cos^{-1}\left(\frac{2}{3\|\mathbf{A}\|\left[1 + (1 - C'/C)\left(\tfrac{2}{3} - \|\mathbf{A}\|^2\right)/\left((\mathbf{A}, \mathbf{A}') - \|\mathbf{A}\|^2\right)\right]}\right). \tag{6.14}$$

In general, we have two sets of solutions due to the multivaluedness of $\cos^{-1}$, and the one which gives a smaller absolute value of Ω must be chosen. This result is obtained on the assumption that $|\Omega|$ is small and has the order of p'^2 or q'^2. However, if $|\Omega|$ is not small compared to p'^2 or q'^2, in other words, if p'^2 and q'^2 are much smaller than $|\Omega|$, the procedure described in the previous section applies. Namely, let $\overline{\Omega} = [\mathbf{A}, \mathbf{A}']/2\|\mathbf{A}\|^2$ be a first approximation of Ω, and transform C', A_2', and B_2' to those of the rotated figure by $-\overline{\Omega}$. Then, the modified motion is expected to have a smaller value of $|\Omega|$. The true p' and q' are obtained by rotating the computed gradient vector (p', q') by $\overline{\Omega}$.

The curve C of Fig. 6 shows the shape of the surface used in Fig. 4 when $p = q = 0$ (i.e., slant 0), and C' is the projected image of the same surface slanted by

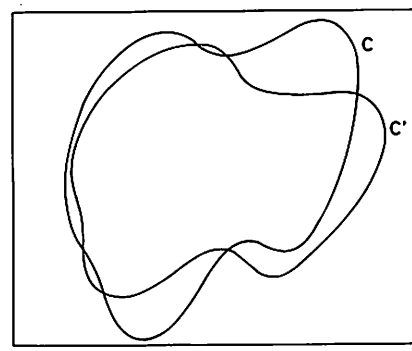

FIG. 6. The shape C of the surface of Fig. 4 with slant 0, and image C' of the same surface slanted by slant 30° and tilt 10° and rotated by −20° about the z axis.

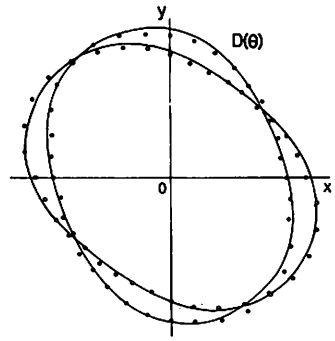

FIG. 7. Diameters of 18 different orientations—white circles for C and black dots for C'. The solid curves are approximations up to the second Fourier harmonics computed from those data.

slant 30° and tilt 10° and rotated by −20° about the z axis. Hence, the true gradients are $p' = -0.289$ and $q' = -0.5$. We measured diameters of 18 different orientations, which are shown in Fig. 7—white circles for C and black dots for C'. The solid curves are approximations up to the second Fourier harmonics. In other words, our scheme regards these curves as the true diameter distributions. Applying the above procedures, we obtain $p' = 0.293$ and $q' = 0.420$, which is again a good estimate in view of the large amount of relative motions and the approximation involved.

7. CONCLUDING REMARKS

The underlying assumption in the present scheme is that we are observing an "orthographically" projected image of a moving "planar" surface of an arbitrary shape having a "closed" contour. The proposed method has the following salient features: (1) There is no need to seek correspondence of points, which saves computation time. (2) All computations involve only three "features" C, A_2, and B_2 measured on the plane of vision, and there is no need to retain the image itself, which saves memory space. (3) The features are "invariant" with respect to translational motions, so that the separation of rotational motions from translational motions is incorporated from the beginning. (4) The computation is stable with respect to local errors, because the features are average quantities of a number of measurements. (5) The surface orientation is given by explicit formulae, and no iterative process is involved, which saves computation time.

A remaining problem is the accuracy, because several types of approximation are used. The accuracy is affected by (i) accuracy of diameter measurement, (ii) the number of orientations along which the diameter is measured, (iii) the magnitude of high harmonics of the distribution density of the convex hull of the contour because we consider only harmonics up to the second order, and (iv) the time interval of measurements because we approximate derivatives by differences. Here, (i), (ii), and (iv) are not serious problems, because they depend on implementation techniques and their effect can be made as small as desired in principle. In contrast, (iii) is characteristic of the surface shape itself. Hence, this scheme is most suitable for those which have "smooth and general" convex hulls without having any corners or special symmetries, but not for too regular shapes like circles and rectangles lacking

a certain range of orientations at all. However, though the prediction may be poor for those shapes, it still gives a rough estimate, since we are comparing two distributions like those in Fig. 7 approximated up to the second order. If we want accuracy, we can resort to the scheme of Kanatani [13] which does not involve any assumption about the shape and hence is exact in principle. However, it fails to give reasonable estimates when the relative motion becomes large, while the present one gives fairly good estimates even when the relative motion is large, as is shown in our examples. Hence, the merits and drawbacks of these two schemes are complementary, one is accurate but sensitive and the other rough but robust. Thus, the present scheme serves many purposes if properly used and combined with other processes. For example, it is a wise policy to make corrections now and then by using iterative processes based on the estimates of the present scheme in order to clear the possible accumulated errors.

ACKNOWLEDGMENTS

Part of this work was supported by Saneyoshi Scholarship Foundation.

REFERENCES

1. H. C. Longuet-Higgins and K. Prazdny, The interpretation of a moving retinal image, *Proc. Roy. Soc. London Ser. B* **208**, 1980, 385–397.
2. K. Prazndy, Egomotion and relative depth map from optical flow, *Biol. Cybernetics* **36**, 1980, 87–102.
3. B. K. P. Horn and B. G. Schunk, Determining optical flow, *Artificial Intelligence* **17**, 1981, 185–203.
4. S. Amari, Invariant structures of signal and feature spaces in pattern recognition problems, *RAAG Memoirs* **4**, 1968, 533–566.
5. S. Amari, Feature spaces which admit and detect invariant signal transformations in, *Proc. 4th Int. Joint Conf. Pattern Recognition*, 1978, pp. 452–456.
6. K. Kanatani, Detection of surface orientation and motion from texture by a stereological technique, *Artificial Intelligence* **23**, 1984, 213–237.
7. L. A. Santaló, *Introduction to Integral Geometry*, Herman, Paris, 1953.
8. M. G. Kendall and P. A. Moran, *Geometrical Probability*, Griffin, London, 1963.
9. L. A. Santaló, *Integral Geometry and Geometrical Probability*, Addison–Wesley, Reading Mass., 1976.
10. K. Kanatani, Stereological determination of structural anisotropy, *Int. J. Engng Sci.* **22-5**, 1984, 531–546.
11. K. Kanatani and O. Ishikawa, Error analysis for the stereological estimation of sphere size distribution—Abel type integral equation, *J. Comput. Phys.* in press.
12. K. Kanatani, Procedures for stereological estimation of structural anisotropy, *Int. J. Engng Sci.*, in press.
13. K. Kanatani, Detecting the motion of a planar surface by line and surface integrals, *Comput. Vision Graphics Image Process.* **29**, 1985, 13–22.
14. K. Kanatani, Distribution of directional data and fabric tensors, *Int. J. Engng Sci.*, **22-2**, 1984, 149–164.